REPORT DOCUMENTATION PAGE

Form Approved
OMB No. 0704-0188

1. REPORT DATE *(DD-MM-YYYY)*
07-16-2013

2. REPORT TYPE
Conference Proceedings

3. DATES COVERED *(From - To)*

4. TITLE AND SUBTITLE
Bathymetry Estimations Using Vicariously Calibrated HICO Data

5a. CONTRACT NUMBER

5b. GRANT NUMBER

5c. PROGRAM ELEMENT NUMBER
0602435N

6. AUTHOR(S)
David Lewis, Richard Gould, Alan Weidemann, Sherwin Ladner and Zhongping Lee

5d. PROJECT NUMBER

5e. TASK NUMBER

5f. WORK UNIT NUMBER
73-6552-03-5

7. PERFORMING ORGANIZATION NAME(S) AND ADDRESS(ES)
Naval Research Laboratory
Oceanography Division
Stennis Space Center, MS 39529-5004

8. PERFORMING ORGANIZATION REPORT NUMBER
NRL/PP/7330--13-1727

9. SPONSORING/MONITORING AGENCY NAME(S) AND ADDRESS(ES)
Office of Naval Research
One Liberty Center
875 North Randolph Street, Suite 1425
Arlington, VA 22203-1995

10. SPONSOR/MONITOR'S ACRONYM(S)
ONR

11. SPONSOR/MONITOR'S REPORT NUMBER(S)

12. DISTRIBUTION/AVAILABILITY STATEMENT
Approved for public release, distribution is unlimited.

13. SUPPLEMENTARY NOTES

14. ABSTRACT
The Hyperspectral Imager for the Coastal Ocean (HICO) is a prototype sensor installed on the International Space Station (ISS) designed to explore the management and capability of a space-borne hyperspectral sensor. The Office of Naval Research (ONR) funded the development and management of HICO. The Naval Research Laboratory (NRL) built and is involved in management of the HICO sensor. Bathymetry information is essential for naval operations in coastal regions. However, bathymetry may not be available in denied areas. HICO has a 100 meter spatial resolution, which makes it more capable for providing information within bays and estuaries than other sensors with coarser resolutions. Furthermore, its contiguous hyperspectral range is well suited to be used as input to the Hyperspectral Optimization Process Exemplar (HOPE) algorithm, which along with other absorption and backscattering values, estimates bottom albedo and water depth. Vicarious calibration uses in situ data to generate new gains and offsets that when applied to the top-of-atmosphere radiance values improves atmospheric correction results and the measurement of normalized water-leaving radiances. In situ remote sensing reflectance data collected in St. Andrews Bay were used to vicariously calibrate a coincident HICO scene. NRL's Automated Processing System (APS) was used to perform atmospheric correction and estimation of remote sensing reflectance (Rrs). The HOPE algorithm used the vicariously calibrated HICO Rrs values to estimate water depth. The results were validated with bathymetry maps from the NOAA National Ocean Service (NOS).

15. SUBJECT TERMS
remote sensing, HICO, HOPE, bathymetry, vicarious calibration, St. Andrews Bay

16. SECURITY CLASSIFICATION OF: a. REPORT	b. ABSTRACT	c. THIS PAGE	17. LIMITATION OF ABSTRACT	18. NUMBER OF PAGES	19a. NAME OF RESPONSIBLE PERSON
Unclassified	Unclassified	Unclassified	UU	12	David Lewis

19b. TELEPHONE NUMBER *(Include area code)*
(228) 688-5280

Reset

Bathymetry estimations using vicariously calibrated HICO data

David Lewis[1], david.lewis@nrlssc.navy.mil
Richard W Gould Jr[1], rick.gould@nrlssc.navy.mil
Alan Weidemann[1], alan.weidemann@nrlssc.navy.mil
Sherwin Ladner[1], sherwin.ladner@nrlssc.navy.mil
Zhongping Lee[2], zhongping.lee@umb.edu

[1]NRL, Code 7331, Building 1009, Stennis Space Center, MS 39529,
[2]University of Massachusetts, Boston, MA 02125

ABSTRACT

The Hyperspectral Imager for the Coastal Ocean (HICO) is a prototype sensor installed on the International Space Station (ISS) designed to explore the management and capability of a space-borne hyperspectral sensor. The Office of Naval Research (ONR) funded the development and management of HICO. The Naval Research Laboratory (NRL) built and is involved in management of the HICO sensor. Bathymetry information is essential for naval operations in coastal regions. However, bathymetry may not be available in denied areas. HICO has a 100 meter spatial resolution, which makes it more capable for providing information within bays and estuaries than other sensors with coarser resolutions. Furthermore, its contiguous hyperspectral range is well suited to be used as input to the Hyperspectral Optimization Process Exemplar (HOPE) algorithm, which along with other absorption and backscattering values, estimates bottom albedo and water depth. Vicarious calibration uses in situ data to generate new gains and offsets that when applied to the top-of-atmosphere radiance values improves atmospheric correction results and the measurement of normalized water-leaving radiances. In situ remote sensing reflectance data collected in St. Andrews Bay were used to vicariously calibrate a coincident HICO scene. NRL's Automated Processing System (APS) was used to perform atmospheric correction and estimation of remote sensing reflectance (Rrs). The HOPE algorithm used the vicariously calibrated HICO Rrs values to estimate water depth. The results were validated with bathymetry maps from the NOAA National Ocean Service (NOS).

Remote Sensing, HICO, HOPE, Bathymetry, Vicarious Calibration, St. Andrews Bay

1 INTRODUCTION

The Hyperspectral Imager for the Coastal Ocean (HICO) sensor was installed on the International Space Station (ISS) in September, 2009. The parameters for HICO data include 128 spectral bands of top-of-the-atmosphere radiance (Lt) data with a spectral resolution from 352 to 1079 nm wavelength. However, the accuracy of the measurement at the ends of this range is affected by the decreasing quantum efficiency of the sensing elements at those locations. Therefore, the effective usable spectral range is from about 400 to 900 nm wavelengths. The spectral band width is 5.7 nm.

The sensor can acquire targets that are less than roughly 35% from the nadir track of the ISS. The spatial resolution of the HICO data depends on the altitude of the ISS. The sensor acquires remote sensing data in the visible and near infrared wavelength range for a 512 column and 2000 row scene. The spatial resolution of the sensor is roughly 100 m and therefore, the geographic extent of the HICO scene is about 51 by 200 km. When compared to the 1 km or 250 m spatial resolution of MODIS, this higher spatial resolution allows HICO data to be used to generate more relevant information within bays and estuaries where physical and bio-optical processes can change over short spatial scales.

After radiometric calibration, the level 1B HICO data contains Lt values as well as sensor and solar zenith and azimuth angles. Gain factors derived from in situ data used in vicarious calibration can adjust top-of-the-atmosphere radiance values to improve in-water measurement accuracy. This vicarious calibration process was used with an in situ data set to explore the ability to refine HICO data measurement.

Ocean Sensing and Monitoring V, edited by Weilin W. Hou, Robert A. Arnone, Proc. of SPIE Vol. 8724,
87240N · © 2013 SPIE · CCC code: 0277-786X/13/$18 · doi: 10.1117/12.2017864

Water depth (bathymetry) in denied areas is important information for mission planning. This is especially true in coastal and riverine environments. Water depth estimated from the hyperspectral bands of HICO data could provide higher spatial resolution and potentially more accurate estimates than the Moderate Resolution Imaging Spectroradiometer (MODIS) data.

The Hyperspectral Optimization Exemplar (HOPE)[1] is an iterative optimization program. This program minimizes an objective function to generate estimates for such products as phytoplankton absorption coefficient at 440nm, absorption coefficient for gelbstoff and detritus at 440nm, particle-backscattering coefficient at 400nm, bottom albedo (reflectance) at 550nm and water depth.

In order to perform water depth estimations, HOPE requires remote sensing reflectance, Rrs, values as input along with each band's wavelength. The parameters fed into the HOPE process identify constraints such as over what wavelength range the optimization process should be performed. Since HICO has contiguous wavelength data at 5.7 nm wavelength integrals, it is well suited to be used as input for HOPE.

2 METHODOLOGY

The methodology in this investigation involved fine-tuning of sensor gains through vicarious calibration. The remote sensing reflectance (Rrs) generated after processing the HICO data with the new sensor gains were then used as input to the HOPE algorithm to estimate water depth, which has previously been used to estimate bathymetry near Freshwater Beach, Australia[2].

2.1 Vicarious Calibration

Vicarious calibration is a flexible process for establishing gain adjustments to improve measurement accuracy of normalized water-leaving radiances (nLw) of HICO data[3]. The nLw values are derived from the Lt values as a result of the atmospheric correction process. While the selected atmospheric correction is being performed various scattering and absorption factors are generated for use in adjusting the Lt value to derive the nLw value for each wavelength band. These include estimations of the Rayleigh and aerosol radiances and atmospheric gas absorption coefficients. After the satellite-derived nLw values have been computed, the various scattering and absorption factors are still held in memory. To perform the vicarious calibration, the satellite-derived nLw values are then replaced by in situ nLw values. All the atmospheric correction scattering and absorption factors held in memory are then added to the in situ nLw values. This results in a vicarious top-of-the atmosphere radiance measurement (vLt) for each wavelength band.

The ratio of the vLt / Lt provides a vicariously calibrated gain factor that, when multiplied to the Lt value, provides the top-of the-atmosphere radiance value needed to derive the in situ nLw values as the satellite-derived nLw measurements. If multiple samples are used, a regression between the samples' Lt and vLt values can be used to generate vicariously calibration gain and offset values for each wavelength band, with the slope of the regression providing the gain and the y-intercept of the regression providing the offset. The samples can be processed again while applying the newly computed gains and offsets to the Lt values. RMS errors can be generated between the new satellite-derived nLw values and the in situ nLw values and compared to RMS errors generated before the application of the new gains in order to assess the improvement in the measurement of nLw.

The near infrared (NIR) wavelength bands are used to determine which aerosol model will be used to establish the aerosol radiance contribution. Therefore, the vicarious calibration process is performed in two passes, with the gains and offsets being computed for the NIR wavelength bands being generated first while assuming a specific aerosol model. Once the gains and offsets are established for the NIR wavelength bands, the second vicarious calibration pass generates gains and offsets for the visible wavelength bands.

The availability of ASD radiometer in situ data on 11/10/12 was used to vicariously calibrate the coincident HICO scene over the St. Andrews Bay near panama City, Florida. A total of 9 in situ data locations (stations) were used in the calibration process. The vLt values were computed for each of the 9 stations.
In order to explore the effect of the derived gains and offsets, the in situ data was partitioned into a set of the even-indexed samples and a set of the odd-indexed samples. Vicarious calibrated gains were generated from each of these two

in situ data sets. New nLw values were derived applying each of these gains and offsets separately to inspect the improvement realized for locations not used in the vicarious calibration training.

A regression between the Lt and vLt for each of these two in situ data sets resulted in gains and offsets to apply to the Lt values that would calibrate them to the vLt values. The Lt and the derived vLt spectral curves for In situ Station 4 and 6 are shown in Figures 1 and 2. These graphs, which depict the difference between the Lt spectra before and after the vicarious calibration, show the Lt spectra converge to the vLt spectra after vicarious calibration step.

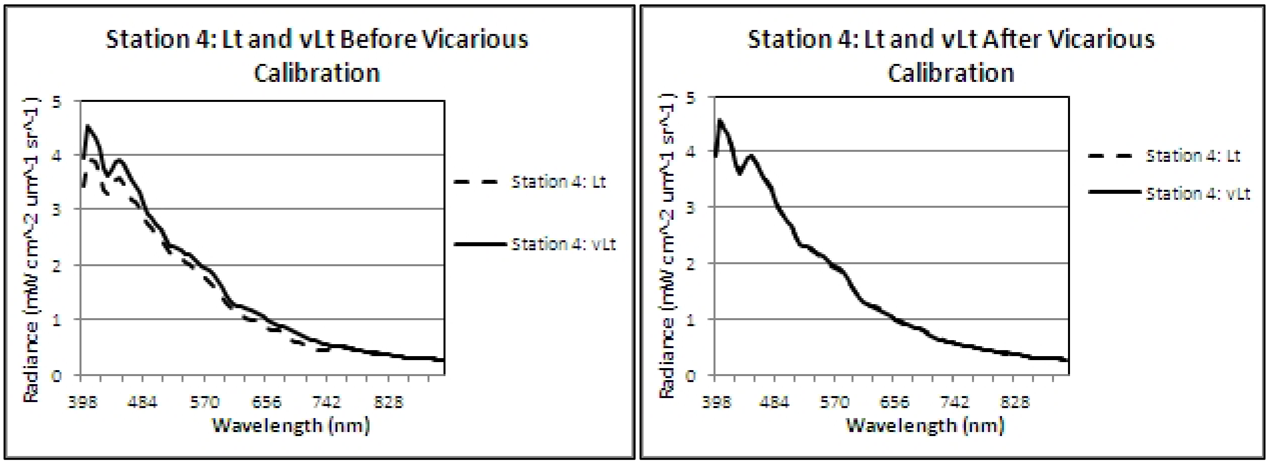

Figure 1. Lt and vLt spectral curves before and after vicarious calibration for Station 4

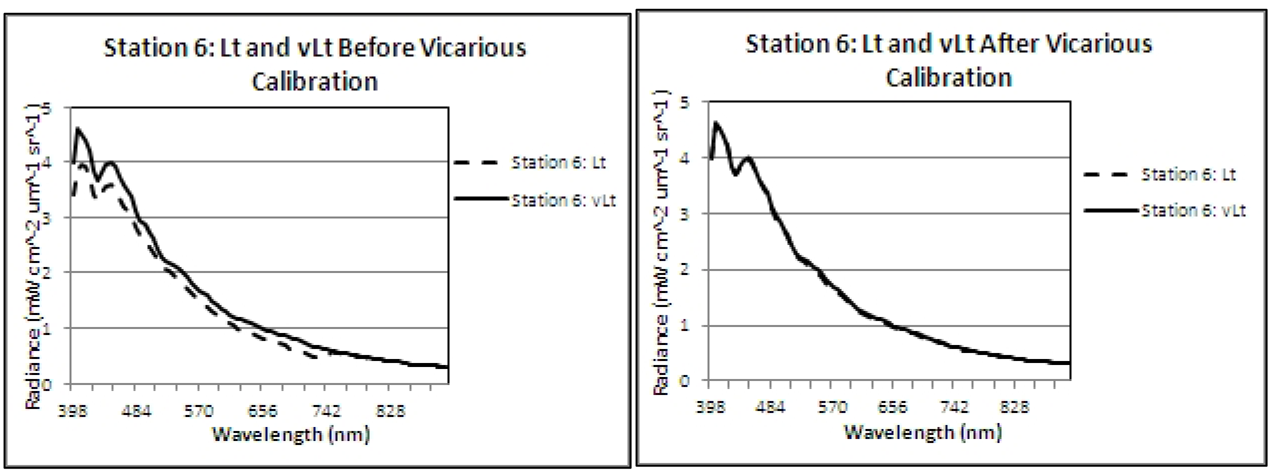

Figure 2. Lt and vLt spectral curves before and after vicarious calibration for Station 6

The new gains were then applied to test sets of HICO data, producing improved satellite-derived nLw values. For example, scatter plots of nLw for the 530 nm wavelength band before and after vicarious calibration is shown in Figure 3. The r^2 values of the scatter plot increased from 0.69 before to 0.75 after the vicarious calibration for the 530 nm wavelength band. Also, the regression slope between the in situ and HICO derived nLw values increased from 0.85 before to 0.97 after vicarious calibration. The absolute value of the y-intercept was reduced by an order of magnitude. This indicates that the vicarious calibration brings the derived nLw spectra for the 530 nm band closer to the 1 to 1 match with the in situ data.

RMS errors between in situ nLw values and the pre and post-calibrated nLw values were generated to provide assessments of the improvement realized through the vicarious calibration process. The “Averaged Sample” nLw RMS error for the HICO even-indexed in situ data set decreased from 0.44 before to 0.05 radiance units after the vicarious adjustment. The “Averaged Sample” nLw RMS error for the HICO odd-indexed in situ data set decreased from 0.50 before to 0.07 radiance units after the vicarious adjustment.

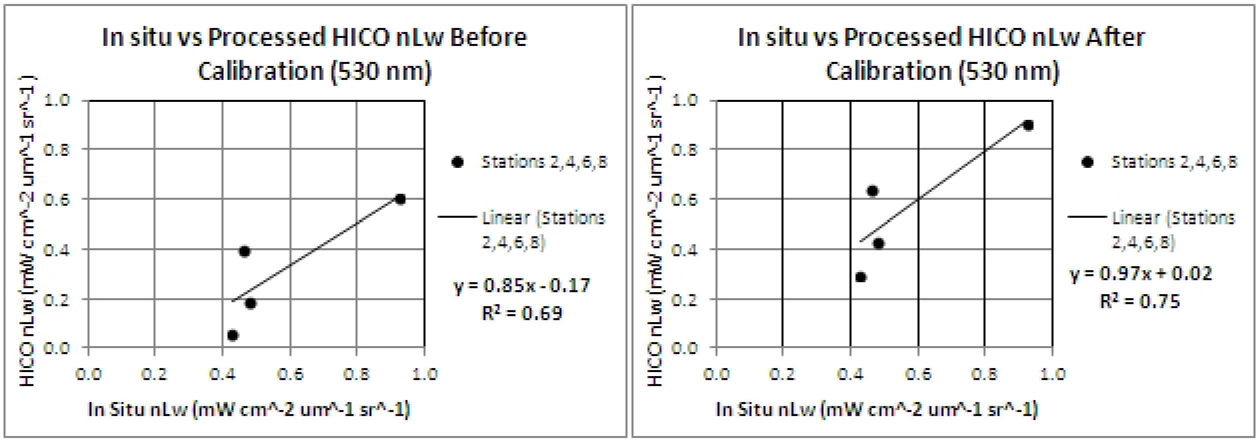

Figure 3. Scatter plot of ASD in situ and HICO nLw values at 530 nm wavelength before and after vicarious calibration

Graphs of the improvement in the nLw spectra for Station 4 are shown in Figure 4 and for Station 6 in Figure 5. In each of these figures, the first graph shows the in situ nLw spectra and the HICO nLw spectra derived with standard gains (i.e., gains of “1” and offsets of “0”). The HICO derived nLw for Station 4 underestimates the in situ nLw, while the derived nLw for Station 6 significantly underestimates the in situ nLw, falling negative for most of the wavelength range.

The second graph of these figures shows the nLw spectra resulting from gains derived from using the set of even-numbered station samples for in situ data in the vicarious calibration process (identified as the “test” set in the graph). This represent the improvement for Stations 4 and 6 using gains which include these stations as in situ data locations in the vicarious calibration. The post calibration derived nLw spectra are significantly closer to the in situ nLw spectra.

The third graph of these figures shows the nLw spectra resulting from gains derived from using the set of odd-numbered station samples for in situ data in the vicarious calibration process (identified as the “training” set in the graph). This represents the improvement for Stations 4 and 6 using gains which do not include these stations as in situ data in the vicarious calibration process. While matching the in situ data better than the nLw spectra derived from standard gains, these nLw spectra deviate from the in situ nLw spectra more than the “test” set graphs. This indicates that the optimal improvement for vicarious calibration is, not surprisingly, realized at the in situ locations which are used to generate the vicarious calibration gains. Since vicarious calibration can provide sensor-derived nLw values that more closely match in situ nLw values and reduce the overall nLw measured RMS error, it proves to be a good method for fine-tuning nLw measurement of HICO data sets.

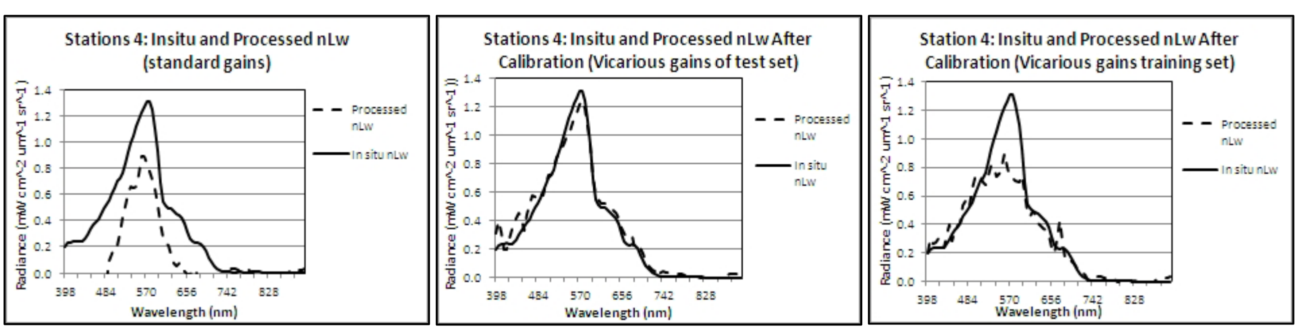

Figure 4. In situ and HICO nLw for a) standard gains, b) even-numbered station gains, c) odd-numbered station gains for Station 4

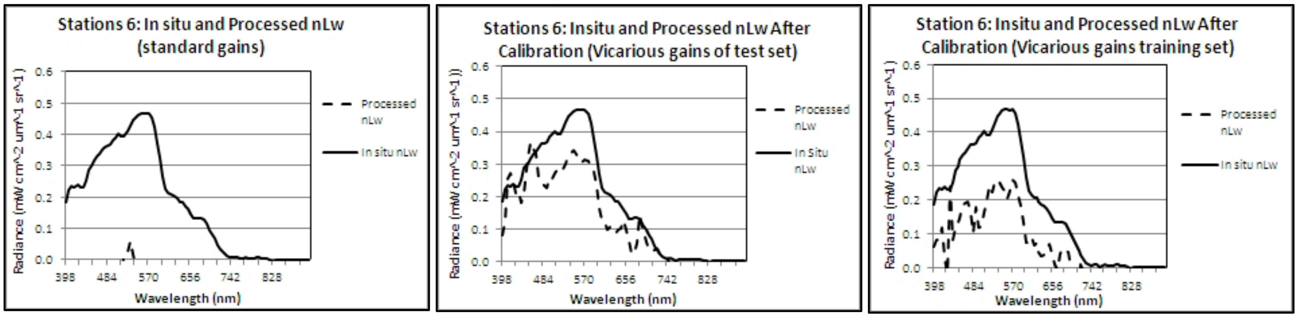

Figure 5. In situ and HICO nLw for a) standard gains, b) even-numbered station gains, c) odd-numbered station gains for Station 6

2.2 Bathymetry Estimation Data Processing

Co-incident in situ data were collected from the NRL "Ocean Color" boat within the St. Andrews Bay on two different occasions. During these data collection missions, water depth from an echo sounder, reflectance measurements from an Analytical Spectral Devices (ASD) Handheld 2 Radiometer, inherent optical properties from a Hyperpro, inherent optical properties from a AC9 sensor, sun photometer data, video from a Gopro camera housed on the AC9 and digital photographs were recorded. The reflectance and water-leaving radiance measurements were used to vicariously calibrate the HICO data. The AC9 data were used to determine water absorption and scattering properties. The video was used to help determine bottom type.

The first in situ data collection mission was on 10/29/12, which was to be co-incident with a HICO overpass. Unfortunately, due to complications resulting from the impact of Hurricane Sandy on the US Northeastern seaboard, the HICO scene was not acquired. However, the water depth acquired from the "Ocean Color" echo sounder on 10/29/12 was used to evaluate an estuarine bathymetry map of St. Andrews Bay, which was available from the NOAA National Ocean Service (NOS). The second date of in situ data collection was 11/10/12, which did coincide with a HICO scene collection. The in situ data from this mission was used in a variety of ways including vicarious calibration of the HICO Lt data.

The NOS Estuarine Bathymetry map[4] for St. Andrews Bay (Figure 6) covers the West Bay, North Bay, East Bay and St. Andrews Bay. It was generated by the Special Projects Office of NOAA/NOS as part of a project to produce user friendly bathymetry for those estuaries that contained more than 80% spatial coverage of digital sounding data. Bathymetry for St. Andrew Bay was derived from eleven surveys containing 93,025 soundings taken primarily between 1983 and 1988. The average separation between soundings was 52 meters. The range of soundings for the eleven surveys was 2.9 meters to -19.0 meters at mean low water. Mean high water values of 0.4 or 0.5 meters were assigned to the shoreline. The data in the bathymetric map used in this report were gridded to 90 meter cells. Bathymetric elevations within these data sets were referenced to the local tidal datum which typically is Mean Lowest Low Water (MLLW) averaged over a 19 year tidal epoch.

The NOS Estuarine Bathymetry map shows that the maximum depth of St. Andrews Bay is almost 14 meters in the channels that runs from the junction of the North Bay and West Bay through the St. Andrews Bay to the East Bay. The southern part of St. Andrews Bay has shallow sand bars that run from the area of the deeper channel toward the East Pass. These shallows can reach less than a meter in some locations. For much of the rest of this discussion, the NOS Estuarine Bathymetric map will be referred to as the bathymetry map or simply the "bathy map".

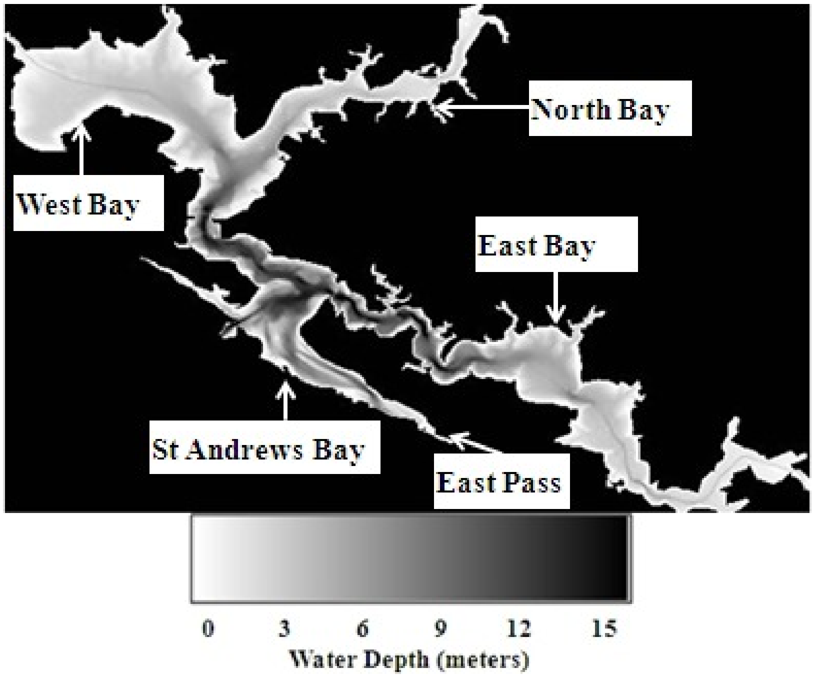

Figure 6. St. Andrews Bay NOS Bathymetry Map

The echo sounder data collected on 10/29/12 was overlain on the bathy map (Figure 7). Water depth values from the bathy map and the echo sounder were extracted and matched together. Points representing echo sounder points that were greater than 5 meters away from the bathy map cell centers were excluded.

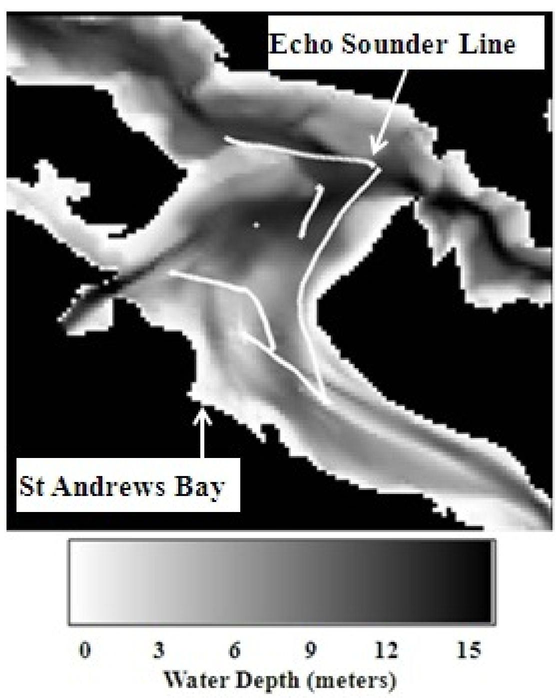

Figure 7. St. Andrews Bay NOS Bathymetry Map with Superimposed Echo Sounder Lines

A scatter plot and regression of the bathy map versus echo sounder water depth were performed. The scatter plot of the bathy map and the in situ water depth data are shown in Figure 8. The echo sounder data was adjusted with recorded tidal information. The r^2 for this data pairing is 0.99 with a regression slope of 1.06. The regression offset of 0.12 meters is within tidal variations during the day.

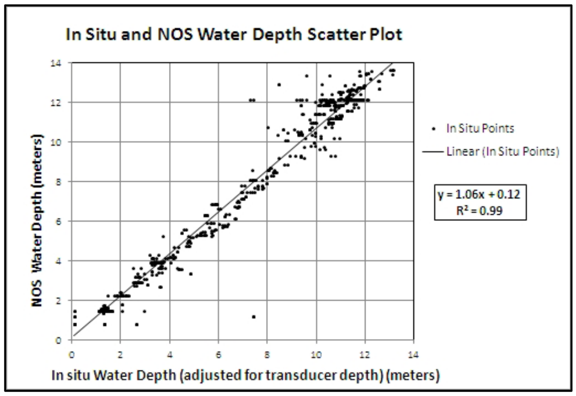

Figure 8. Scatter plot of in situ water depth versus NOS Bathymetry map water depth

The r^2 between the bathy map and echo sounder sample point water depth is highly significant. Therefore, the echo sounder data validates the bathy map and indicates that the water depths derived from the bathy map were adequate for comparisons with the HICO-derived bathymetry estimates. For the remaining data analysis the NOS Bathymetry map will be used to represent the water depth within the entire extent of St. Andrews Bay.

HICO data was collected over the St. Andrews Bay near Panama City, Florida on 11/10/12, which was the second day of in situ data collection. The atmosphere was relatively clear. As with other HICO scenes the raw data was processed by NRL to Level 1B, which computes the top-of-atmosphere radiance, Lt, values. The NRL Automated Processing System (APS) was used to perform atmospheric correction, which resulted in the estimation of normalized water-leaving radiance, nLw, values. The Rrs values were computed from nLw by Equation 1.

Rrs = nLw / f0, where f0 is the solar irradiance Equation 1

The atmospheric correction of the HICO data collected on 11/10/12 was performed by the Gordon-Wang method included in APS, which is a standard NASA ocean color atmospheric correction scheme for sensors including Sea-viewing Wide Field-of-view (SeaWiFS) and MODIS[5]. The process converts the Lt values to nLw values. As described previously, the availability of the ASD reflectance and the Hyperpro nLw values provided the opportunity to vicariously calibrate the HICO scene. This process requires in situ nLw data to adjust HICO Lt values. The ASD reflectance data can be converted to nLw values through inverting Equation 1 and using recorded solar irradiance (f0) data.

This vicarious calibration process described in the previous section was performed using both the ASD and Hyperpro data. The results in this report will use data products from the 11/10/12 HICO data processed using vicariously calibrated gains generated using the coincident in situ ASD radiometer data collected on the same day as the HICO imagery. The vicarious calibration process used all 9 in situ stations to generate the new gains used to reprocess the 11/10/12 HICO scene.

Various APS products, including Rrs and nLw for the HICO wavelength range, were generated using the vicariously calibrated gain settings. The Rrs values generated by APS were smoothed by a 3x3 weighted average and then used as input to HOPE. The HOPE process generated the phytoplankton absorption coefficient at 440nm, absorption coefficient for gelbstoff and detritus at 440nm, particle-backscattering coefficient at 400nm, bottom albedo (reflectance) at 550nm and water depth.

The bathy map was used as a basemap in order to georeference the HICO Lt scene within ENVI. The final ground control points used in this georeference were stored and then used to georeference both the APS and HOPE products.

Figure 9 shows the bathy map of St. Andrews Bay with a land mask generated from a threshold on a NIR Lt value. Figure 10 shows the map of the HOPE water depth estimates for the same extent.

Similar features appear along the shallows found in the southern section of the image. However the HOPE computes shallow depths in the nothern part of the where the bathy map records deeper values. This corresponds to areas where the HOPE bottom reflectance is less than 0.001; areas where the water depth is too deep, or the optical properties are too high to retrieve an adequate bottom reflectance signal for the HOPE inversion process. Therefore, it is concluded that if HOPE doesn't have a resonable bottom reflectance signal, then the confidence in its water depth estimate accuracy is low.

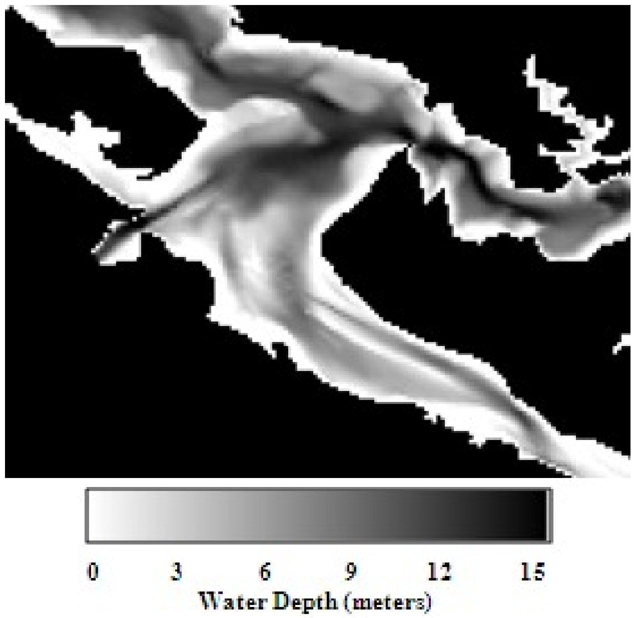

Figure 9. NOS Bathymetry Map with Land Mask

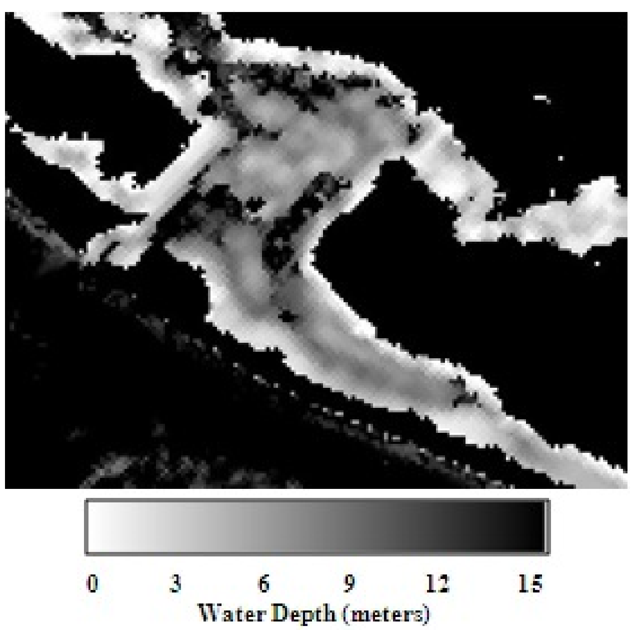

Figure 10. HOPE Water Depth Map with Land Mask

A threshold of 0.001 on the bottom reflectance was used to generate an “invalid data” mask (i.e., to mask areas where we consider the HOPE-derived bathymetry estimates to be invalid). The mask was used to identify the locations of invalid HOPE water depth pixels of the bathy map in Figure 11 and for the map of the HOPE water depth estimates in Figure 12. It can be seen that this removes much of the areas of difference between the two images. Comparison of these figures with Figures 9 and 10 shows that many of the pixels in the invalid data mask coincide with pixels with water depth greater than about 9 meters. Most of the pixles that have water depth greater than about 9 meters, but that are not in the invalid data mask, have bottom reflectance close to but not less than the invalid data threshold of 0.001.

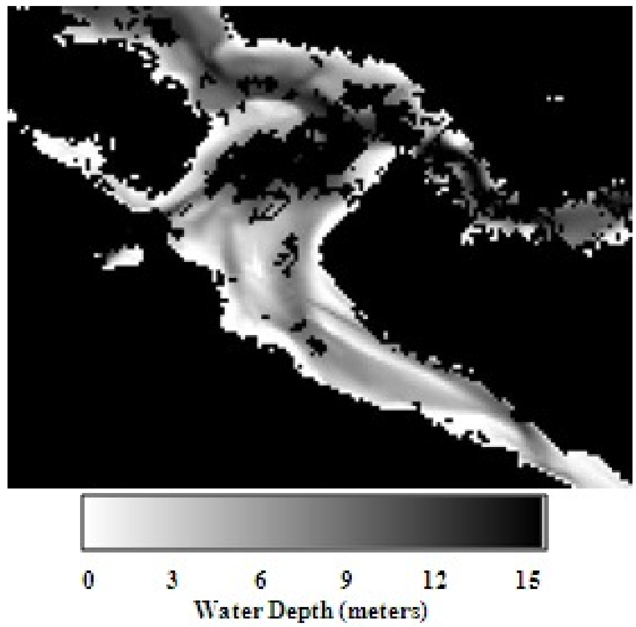

Figure 11. NOS Bathymetry Map with HOPE invalid data mask

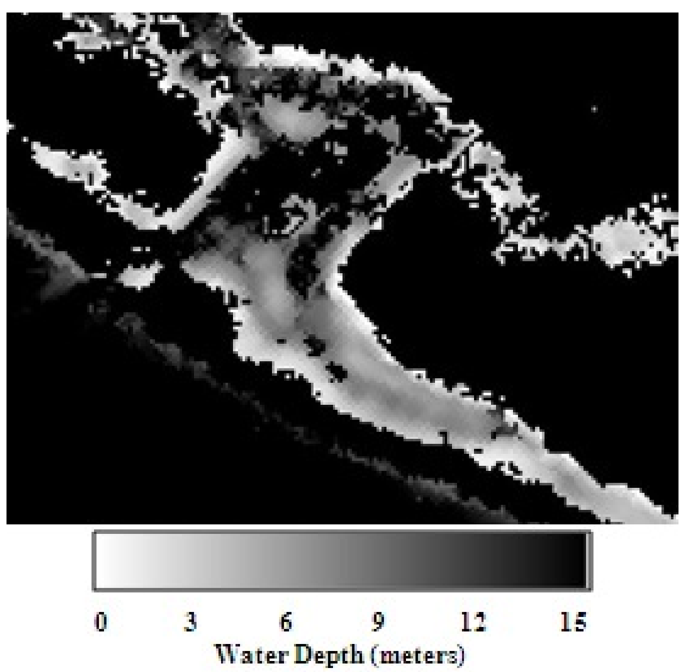

Figure 12. HOPE Water Depth Map with HOPE invalid data mask

Random points were selected in the southern region of St. Andrews Bay outside the land and invalid data mask areas. These points are shown as white dots within both the image of the bathy map and the HOPE water depth masks in Figures 13 and 14. Water depth values were extracted from both of these maps at the sample point locations to create a pairing of water depth measurements.

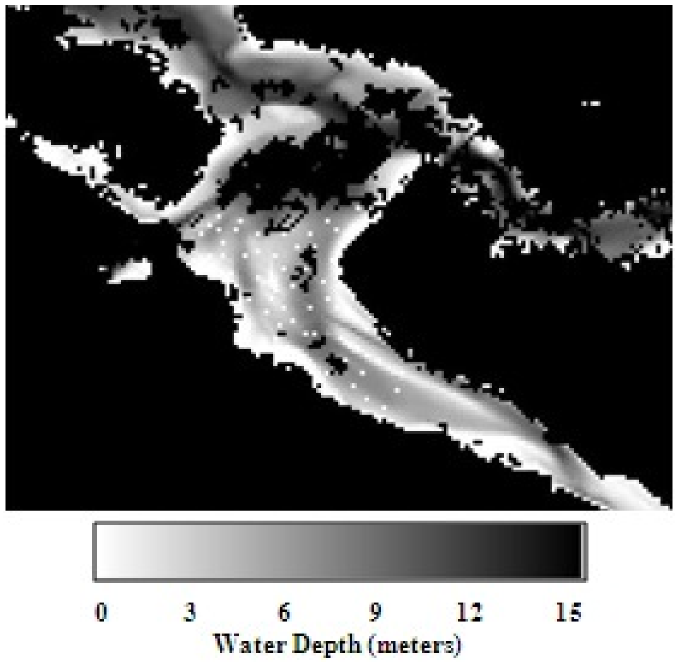

Figure 13. NOS Bathymetry Map with sample point locations (white dots)

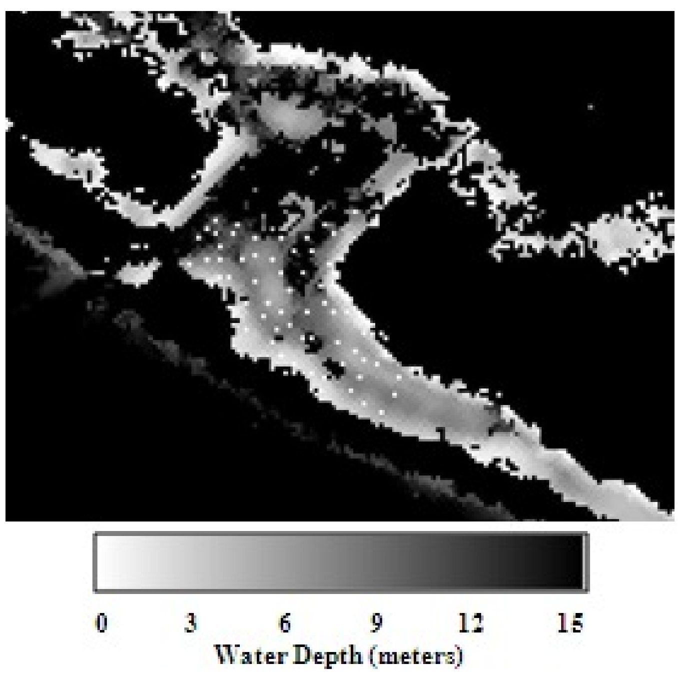

Figure 14. HOPE Water Depth Map with sample point locations (white dots)

A scatter plot between the bathy map and HOPE water depth data drawn from the sample point locations was created. Figure 15 shows the scatter plot and associated regression line. The regression slope is 0.86 and the r^2 for this data pairing is 0.65, which is a reasonable correlation for estimation of water depth.

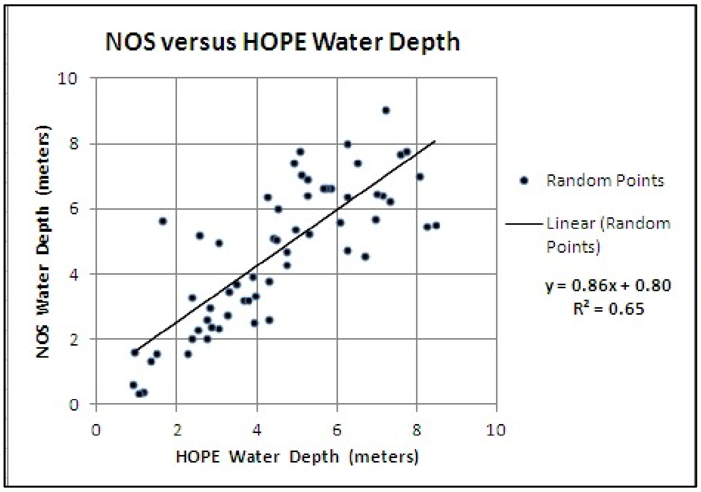

Figure 15. NOS Bathymetry Map and HOPE Water Depth Scatter Plot

3 SUMMARY AND CONCLUSION

Vicarious calibration used in situ data to establish gains for adjusting Lt values so that they more accurately retrieve the known nLw values. APS has the ability to invert the atmospheric correction process for an individual pixel to estimate its vicarious Lt (vLt). This vLt value is the top-of-the-atmosphere radiance value that is required to derive the in situ nLw values after the atmospheric correction process is complete. Additional software was developed to create a system for feeding in situ data into this atmospheric correction inversion and to generate gains from the regression of the resulting vLt on the Lt data.

ASD radiometer in situ data was used to vicariously calibrate HICO data over St. Andrews Bay. APS used the vicariously calibrated gains to perform atmospheric correction and generate nLw values. The nLw values were used to generate Rrs values which were then used by HOPE to estimate water depth.

NOS bathymetry data was validated as accurate ground truth using echo sounder data across several transects in St. Andrews Bay. The NOS bathymetric map was used as a base map to georeference the HICO products and the resulting HOPE water depth product.

For the 11/10/12 HICO scene the bottom reflectance less than 0.001 corresponded with areas of water depth greater than 9 meters. These areas had bottom reflectance too low to provide reasonable water depth estimates. Randomly selected points were generated within an area with bottom reflectance greater than 0.001. The r^2 between the HOPE-derived water depth and the NOS bathymetry map at these randomly selected points was 0.65.

These results show that HOPE can produce reasonable estimates of water depth. However, when there is no bottom reflectance contained in the Rrs spectra, HOPE's accuracy decreases. This is not unreasonable since without bottom reflectance HOPE has no input to guide estimation of the actual depth. HOPE does provide an estimate of the bottom reflectance which can be used as a measure of confidence. As the value of the bottom reflectance decreases, the confidence in the water depth estimate also decreases.

4 FUTURE WORK

Estimations of water depth using HICO and HOPE can be expanded to be performed periodically in the waters around St. Andrews Bay to identify variations in the HOPE derived water depth measurement over time. Also, vicariously calibrated gains from the MOBY[6] and AERONET[7] sensors as well as in situ data can be used by APS to compute Rrs values. HOPE can use the Rrs values computed from these different gains to generate water depth estimates. The accuracy of the water depth estimates using these different Rrs configurations can be examined to determine confidence intervals at different times of the year and using global and local in situ data.

6 REFRENCES

[1] Lee, Z., Carder, K. L, Mobley, C.D., Steward, R. O., Patch, J. S., "Hyperspectral Remote Sensing for Shallow Waters: 2. Deriving Bottom Depths and Water Properties by Optimization", Applied Optics, 38(18), pp. 3831-3843, 1999

[2] Lewis, D., Arnone, R., Gould, R., Weidemann, A, Ladner, S., Amin, R., Patterson, K., Lamela, G., Casey, B., and Lee, Z., "Bathymetry Estimations Using the Hyperspectral Imager for Coastal Oceans (HICO)Data", Proceedings of AGU 2012 Ocean Science Meeting, 2012

[3] Franz, Bryan A., Bailey, Sean W., Werdell, P. Jeremy, and McClain, Charles R., "Sensor-independent approach to the vicarious calibration of satellite ocean color radiometry", Applied Optics, Vol. 46, No. 22, 1 August 2007

[4] NOAA National Ocean Service, http://estuarinebathymetry.noaa.gov/bathy_htmls/G110.html

[5] Gordon, H. R., Wang, M., "Retrieval of water-leaving radiance and aerosol optical thickness over the oceans with SeaWiFS: a preliminary algorithm", Applied Optics, Vol. 33, No. 3, 20 January, 1994

[6] Clark, Dennis K., Feinholz, Michael E., Yarbrough, Mark A., Johnson, B. Carol, Brown, Steven W., Kim, Yong Sung, and Barnes, Robert A., "Overview of the Radiometric Calibration of MOBY", Proceedings of SPIE Vol. 4483, 2002

[7] Lewis, D., "Vicarious Calibration of the Hyperspectral Imager for Coastal Oceans (HICO) Using MOBY and AERONET-OC Data," Proceedings of 2012 Ocean Optics Conference, 2012